TU/e EINDHOVEN UNIVERSITY OF TECHNOLOGY

Computation of the Infrared spectrum of an acidic zeolite proton interacting with acetonitrile

Citation for published version (APA):
Meijer, E. L., Santen, van, R. A., & Jansen, A. P. J. (1996). Computation of the Infrared spectrum of an acidic zeolite proton interacting with acetonitrile. *Journal of Physical Chemistry*, *100*(22), 9282-9291. https://doi.org/10.1021/jp951164i

DOI:
10.1021/jp951164i

Document status and date:
Published: 01/01/1996

Document Version:
Publisher's PDF, also known as Version of Record (includes final page, issue and volume numbers)

Please check the document version of this publication:

• A submitted manuscript is the version of the article upon submission and before peer-review. There can be important differences between the submitted version and the official published version of record. People interested in the research are advised to contact the author for the final version of the publication, or visit the DOI to the publisher's website.
• The final author version and the galley proof are versions of the publication after peer review.
• The final published version features the final layout of the paper including the volume, issue and page numbers.

Link to publication

General rights
Copyright and moral rights for the publications made accessible in the public portal are retained by the authors and/or other copyright owners and it is a condition of accessing publications that users recognise and abide by the legal requirements associated with these rights.

• Users may download and print one copy of any publication from the public portal for the purpose of private study or research.
• You may not further distribute the material or use it for any profit-making activity or commercial gain
• You may freely distribute the URL identifying the publication in the public portal.

If the publication is distributed under the terms of Article 25fa of the Dutch Copyright Act, indicated by the "Taverne" license above, please follow below link for the End User Agreement:

www.tue.nl/taverne

Take down policy
If you believe that this document breaches copyright please contact us at:

openaccess@tue.nl

providing details and we will investigate your claim.

Download date: 26. Oct. 2021

Computation of the Infrared Spectrum of an Acidic Zeolite Proton Interacting with Acetonitrile

E. L. Meijer,* R. A. van Santen, and A. P. J. Jansen

Eindhoven University of Technology, Schuit Institute of Catalysis, Theory Group, P.O. Box 513, 5600 MB Eindhoven, The Netherlands

Received: April 25, 1995; In Final Form: August 7, 1995[⊗]

The influence of acetonitrile adsorption on the infrared spectrum of an acidic OH group inside a zeolite is studied by theoretical calculations. The zeolite is modeled by a cluster molecule. Potential energy and dipole surfaces of the stretch and two bending coordinates of the acidic H atom, and for the complex with acetonitrile, of an additional acetonitrile stretch coordinate, are computed employing Hartree−Fock as well as density functional methods. Infrared frequencies as well as absorption intensities are computed taking into account mechanical as well as electric anharmonicities up to fourth order. Fermi resonance proposed as the cause of the splitting of the OH stretch absorption bands in infrared spectra is explicitly considered.

Introduction

The infrared spectrum of an XH group in a molecule, where X is typically O, S, F, Cl, Br, or I, can change radically upon hydrogen bonding to some base B. In many different systems the following changes are observed. The XH stretching frequency is lowered considerably, the absorption intensity of the band is enhanced greatly, and the band is broadened by a large amount. In a number of cases the hydrogen-bonded XH stretch band is split into two or more bands. All of the described phenomena appear to be stronger if the acidity of the XH group is greater or if the basic character of B is stronger.

The system under study in the present work is a Brønsted acidic OH group of a zeolite interacting with a molecule of acetonitrile. This system is especially interesting because it exhibits a very large OH stretch frequency shift and also the splitting of the shifted OH stretch band. In the case of adsorption of methanol in a zeolite, a similar multiple-band structure has been found. Kubelková *et al.*[1] have argued that the two bands around 2400 and 2900 cm^{-1} were due to two different structures, in one of which the proton is transferred to the methanol, and in the other it is not. The same bands have been interpreted by Mirth *et al.*[2] as originating from a symmetric and an asymmetric bending of the two hydrogen atoms of the protonated hydroxyl group of methanol. Obviously, this explanation cannot be used for the similar bands of a Brønsted acidic zeolite with acetonitrile around 2400 and 2800 cm^{-1}. In liquids broadening of the XH stretch bands upon hydrogen bonding has been explained from the coupling with XH···B intermolecular stretch modes.[3−5] Splitting of the XH stretch bands has been explained by Fermi resonances of overtones of XH bending modes.[3,5] On the basis of a comparison of the in-plane bending modes of an acidic OH group in a zeolite and peak minima in the infrared spectrum, Pelmenschikov *et al.*[6] proposed a Fermi resonance of the downward shifted OH stretch mode and the upward shifted in-plane bending overtone.

To examine these models in more detail, in the current paper we present calculations of vibrational frequencies and infrared absorption intensities including anharmonicities. Vibrational wave functions are computed for the stretch and bending modes of an acidic proton in a zeolite, and of such a proton with an adsorbed molecule of acetonitrile, where the coupling of the proton modes with the stretch mode of the acetonitrile molecule as a whole with respect to the OH group was included. Anharmonic terms up to fourth order in the potential energy were included, and infrared absorption intensities were computed using a fourth-order dipole surface. The vibrational wave functions were computed in a variational approach. The potential energy and dipole surfaces were fitted to quantum chemical calculations using polynomials.

Theory

The Potential Energy and Dipole Surfaces. The computation of the potential energy and dipole surfaces has been done at the Hartree−Fock level of theory (SCF) and also using density functional theory (DFT). The density functional applied was Becke's three-parameter functional with the nonlocal correlation provided by the Lee, Yang, and Parr expression.[7−10] DFT is assumed to yield results that are closer to experiment, for the energy as well as for the dipole surface.[11] Since the computed infrared spectra from the SCF data and the DFT data were qualitatively very similar, the DFT results are presented completely and only in some cases supplemented by the SCF results.

The cluster approach has been used to model the acidic site of the zeolite. We have used a relatively small cluster, to allow for electronic structure calculations with a reasonably good basis set. The cluster contained the acidic Al(OH)Si group with the dangling bonds of Al and Si saturated by OH groups. A restricted geometry optimization has been done for this cluster, with and without an interacting molecule of acetonitrile, to obtain reference points for the potential energy and dipole surfaces. Full optimization of the geometry of the cluster was not done for two reasons.

Firstly, the cluster molecule forms internal hydrogen bridges between the terminating OH groups. These hydrogen bridges affect the (Al−O−Si) angle, and hence the OH frequency, in a way that is not found in zeolite systems, which we attempt to model. To prevent internal hydrogen bridging, we have optimized the zeolite cluster without acetonitrile with the (Si−O−H) and (Al−O−H) angles of the terminating OH groups fixed at tetrahedral angles and required that, going from the central O atom to a terminal OH, the atoms O−T−O−H (T = Si or T = Al) should be in one plane.

The second reason not to optimize fully has been computational cost. We have imposed C_s symmetry, with the Al(OH)Si

[⊗] Abstract published in *Advance ACS Abstracts,* February 1, 1996.

S0022-3654(95)01164-6 CCC: $12.00 © 1996 American Chemical Society

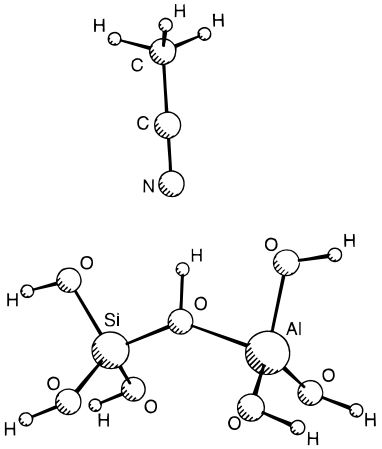

Figure 1. Zeolite cluster with acetonitrile, optimized using DFT.

TABLE 1: Main Results of Geometry Optimizations[a]

	zeolite cluster without acetonitrile		zeolite cluster with acetonitrile		change after absorption	
	SCF	DFT	SCF	DFT	SCF	DFT
r(OH)	0.957	0.979	0.977	1.020	+0.020	+0.041
r(SiO)	1.657	1.673	1.635	1.647	−0.022	−0.026
r(AlO)	1.950	1.966	1.895	1.910	−0.055	−0.056
∠(AlOSi)	140.7	142.9	139.4	141.6	−1.3	−1.3
∠(AlOH)	101.4	97.5	105.0	104.4	+3.6	+6.9
∠(SiOH)	117.9	119.6	115.6	114.4	−2.3	−5.6
r(ON)			2.843	2.701		
∠(HON)[b]			7.7	6.7		

[a] Some geometrical parameters of the central Al−OH−Si group of the zeolite cluster and the N atom of the acetonitrile molecule are given. Distances *r*(...) are in angstrom, angles in degrees. The columns denoted SCF give the Hartree−Fock results; those denoted DFT, the density functional theory results. [b] Acetonitrile bends toward the Si side of the cluster.

part of the cluster positioned in the mirror plane. This has allowed for a considerable reduction of the number of points to be computed for the potential energy surface, as both sides of the mirror plane are equivalent.

In the optimization of the geometry of the zeolite cluster interacting with acetonitrile, we have fixed the terminal OH groups to the positions found in the optimization of the free zeolite cluster, attempting to model the "rigidity" of the zeolite lattice. The acetonitrile has been positioned with the CN group pointing toward the acid OH group, as shown in Figure 1. This mode of adsorption is energetically the most favorable. The two C atoms and the N atom of acetonitrile have been kept fixed on one line. As a result of the optimization, no proton transfer of the zeolite cluster to the acetonitrile has been observed nor has a local minimum in the energy for a proton position closer to the actonitrile than to the zeolite cluster been found. A number of geometrical parameters obtained in the optimizations is given in Table 1.

The basis used to compute the potential energy surface has been chosen so as to give a good description of the near environment of the acidic H atom. At the borders of the zeolite cluster a minimal basis set has been used to reduce computational cost. A STO-3G basis set[12] has been used for the H atoms of the terminating OH groups. We have used a 6-31G** basis set[13−16] for the O atoms of the terminating OH groups, for Si, Al, and the acidic H of the zeolite cluster, and for the C and H atoms of the acetonitrile. For the central O atom of the zeolite cluster and the N atom of acetonitrile, a 6-311+G* basis set has been employed, which provides a good description of the proton affinity of anions.[17−19] From the results in ref 19, the proton transfer from H_2O to NH_3 can be computed to become less unfavorable when going from a double- to a triple-ζ basis set and adding diffuse functions. This effect can be ascribed to the better description of anionic oxygen. Since the interaction between the acidic OH and acetonitrile under study in the current article resembles the beginning of a proton transfer from an oxygen atom to a nitrogen atom, we expect that the used basis set will result in a stronger calculated interaction. Further on in the paper it will be shown that yet a stronger interaction is needed to account for the experimentally observed spectra.

Recently, Haw *et al.*[20] have done a number of SCF geometry optimizations where the acetonitrile molecule has been forced at a more acute angle with the acidic OH in order to model the spatial limitations within a zeolite. We do not feel that changing this angle would have any essential influence on our current results, because the potential of the bending of the acetonitrile molecule as a whole is rather flat.

The potential energy and dipole surfaces of the zeolite cluster without acetonitrile adsorbed have been computed as a function of the acidic H position. The grid we have used to compute potential energy and dipole surfaces has been designed to cover the area in coordinate space where the vibrational wave functions have non-negligible amplitude, i.e., where the potential energy is relatively low. This leads to a description where the grid is closer spaced in areas where the potential energy is changing strongly in a certain direction, e.g., for shorter OH distances. The energy and dipole have been computed at five different OH distances: 0.8, 0.9, 1.0, 1.1, and 1.4 times the equilibrium distance listed in Table 1. For each of these OH distances, the H atom was bent toward the Al atom by an angle θ of 0°, 7.5°, 20°, and 60° and subsequently rotated around the axis defined by the equilibrium OH bond by an angle ϕ of 0°, 45°, 90°, 135°, and 180°. The number of points for which an electronic structure calculation has been done is 80. The values of 45 points corresponding to angles ϕ of 225°, 270°, and 315° have been derived taking the symmetry plane of the cluster into account, adding up to a total of 125 points.

The energy and dipole surfaces of the zeolite cluster with acetonitrile adsorbed have been scanned in the same way as those of the "bare" zeolite cluster with respect to the H positions. For each of the 80 hydrogen positions, the energy and dipole have been computed at five different acetonitrile positions. The acetonitrile molecule has been moved as a whole along its N≡C−C axis found in the equilibrium geometry, with O−N distances of the equilibrium value listed in Table 1, and the equilibrium value plus and minus 0.15 Å and plust and minus 0.5 Å. The total number of points for which an electronic structure calculation has been done for this complex is 400. After addition of symmetrically equivalent points we obtained 625 points of the potential energy and dipole surfaces. All electronic structure calculations were done with the Gaussian 92/DFT[21] program package.

Fit of the Potential Energy and Dipole Surfaces. In the fit of the potential energy, different weights were applied to the different points of the potential energy. The weight factors w_i were chosen in such a way that points with lower energy made a larger contribution to the fit:

$$w_i \equiv \frac{e^{-fv_i}}{\sum_j^N e^{-fv_j}} \qquad (1)$$

where $1/f$ can be viewed as a "characteristic energy", and v_i is the electronic energy of one of the N computed points of the

TABLE 2. Selected Expectation Values of Acidic Proton with Acetonitrile[a]

level	$\langle x_1 \rangle$	Δx_1	$\langle x_2 \rangle$	Δx_2	$\langle x_3 \rangle$	Δx_3	$\langle x_4 \rangle$	Δx_4
0000	0.003	0.080	0.004	0.120	0	0.146	0.002	0.059
0001	0.000	0.080	0.008	0.121	0	0.146	0.029	0.103
0002	−0.002	0.080	0.012	0.122	0	0.147	0.058	0.134
0010	−0.014	0.081	0.009	0.116	0	0.239	0.013	0.060
0020	−0.027	0.086	0.013	0.115	0	0.289	0.022	0.062
0100	−0.004	0.082	0.013	0.203	0	0.140	0.008	0.060
0200	−0.007	0.091	0.017	0.247	0	0.137	0.012	0.061
1000	0.044	0.139	−0.008	0.165	0	0.143	−0.030	0.079

[a] The "level" column shows the quantum numbers of the basis function with the largest coefficient for the involved states; the first quantum number refers to the OH stretch, the second to the in-plane bending, the third to the out-of-plane bending, and the fourth to the acetonitrile stretch. For each of these coordinates, the expectation value and the root mean square displacement $\Delta x \equiv \sqrt{\langle x^2 \rangle - \langle x \rangle^2}$ is given in angstrom. The symbols x_1, x_2, x_3, and x_4 denote the OH stretch, in-plane bending, out-of-plane bending, and acetonitrile stretch displacement coordinates. They have a value of 0 for the equilibrium geometry. For the two stretches (x_1 and x_4), a positive expectation value means that the distance between the zeolite cluster and the H and acetonitrile, respectively, is larger than in the minimum energy geometry.

potential energy surface. The *x*, *y*, and *z* components of the dipole surface were each fitted using the same procedure and the same weight factors $\{w_i\}$ as applied to the corresponding potential energy points. The fits were made using singular value decomposition,[22] so that near-singularities could be removed. To this effect, we had to set one of the singular values to zero for all fits.

The points computed for each potential energy surface had energy values in an interval of approximately $0.2E_h$. To yield a root mean square error smaller than $1 \times 10^{-3}E_h$ for each potential energy fit, the parameter *f* from eq 1 was given a value of $125E_h^{-1}$. This results in a much higher weight for the points of the potential energy near the minimum. By computation of expectation values of coordinates, and of squares of coordinates, we found that the wave functions that were of interest for the current research only had non-negligible amplitudes in an area near the energy minimum. Some of these expectation values can be found in Table 2.

For both three- and the four-dimensional potential energy surfaces, we found that the coefficient of the fourth-order term in the OH stretch coordinate was negative. This implies that there will be nonphysical eigenstates of the Hamiltonian that will be found if the basis functions used extend into the area of the coordinate space where the polynomial describing the potential energy goes to minus infinity. In the basis set we used, this was not a problem, again due to the fact that the wave functions of interest were mostly restricted to an area near the potential energy minimum; thus, no basis functions were needed that extended beyond the sampled coordinate space.

Dynamics. For the vibrational calculations we have described the molecular systems by a set of linear coordinates that facilitate the interpretation of the vibrational states in terms of stretch and bending modes. The OH stretch coordinate describes the movement of the acidic H along the equilibrium OH bond. The in-plane bending coordinate describes the movement of the acidic H perpendicular to the OH stretch coordinate, in the (Al−O−Si) plane of the cluster. The out-of-plane bending coordinate describes the movement perpendicular to the OH stretch coordinate and perpendicular to the (Al−O−Si) plane of the cluster as well. Finally, in the calculations with acetonitrile, the acetonitrile stretch coordinate describes the movement of the acetonitrile molecule as a whole with respect to the zeolite cluster, along its (C−C≡N) axis.

In the computation of the kinetic energy, all atoms of the zeolite cluster, except for the acidic H, were kept fixed. The Hamiltonian is given by[23]

$$H = {}^1/_2 \sum_{i=1}^{D} \sum_{j=1}^{D} M_{ij}^{-1} p_i p_j + \sum_{\alpha_1,\ldots,\alpha_D} a_{\alpha_1,\ldots,\alpha_D} \prod_{i=1}^{D} q_i^{\alpha_i}, \quad \text{with } 0 \le \sum_{i=1}^{D} \alpha_i \le n \quad (2)$$

where *D* is the number of internal coordinates q_i with conjugated momenta p_i, $\mathbf{M}^{-1}$ is the inverse mass matrix, and the $a_{\alpha_1,\ldots,\alpha_D}$ are the coefficients of the polynomial describing the potential energy. The order *n* of the potential energy polynomial was four in the computations in this paper. The way in which the polynomial is truncated ensures that the shape of the potential energy surface does not depend on a particular choice of internal coordinates. Advantages of a polynomial as a functional form are that it has no bias toward the shape of the potential energy, it generates a sparse Hamiltonian matrix in the basis set we employed, and it allows for efficient analytical computation of matrix elements. A disadvantage is the unphysical behavior beyond the area in the internal coordinate space where the fit was made. This can lead to low energies for basis functions of high order due to their having a non-negligible amplitude in an area where the value of the polynomial goes to minus infinity. Such basis functions should be avoided. The cross terms $M_{ij}^{-1}p_ip_j$ in the kinetic energy can have nonzero values if the internal coordinates used are not orthogonal (which is not the case in the current paper).

To find the eigenvalues of the vibrational Hamiltonian, we applied the linear variational principle in which the wave function is expanded in products of one-dimensional harmonic eigenfunctions (Hermite functions).[24]

$$\psi(q_1, \ldots, q_D) = \sum_{\alpha_1,\ldots,\alpha_D} c_{\alpha_1,\ldots,\alpha_D} \prod_{i=1}^{D} \phi^{(\alpha_i)}(q_i) \quad (3)$$

In this expression ψ is the vibrational wave function in *D* dimensions, and $\phi^{(\alpha_i)}(q_i)$ is the normalized α_i^{th} order Hermite function of coordinate q_i. This is similar to the method used by Mijoule *et al.*[25] One-dimensional harmonic eigenfunctions are characterized by the ratio of a mass and a force constant. For the mass of the one-dimensional components of the basis functions, we used the diagonal elements of the inverse mass matrix (M_{ii}^{-1} in eq 2) in our internal coordinate description. The force constants associated with the Hermite functions can be derived from the curvature at the coordinate origin of the potential energy surface in the direction of the corresponding internal coordinate, provided the coordinate origin represents a minimum in this direction. In the present work this was mostly the case, except for the out-of-plane bending coordinate of the acidic proton without acetonitrile, which will be discussed in the Results and Discussion section.

The vibrational basis set used for the acidic proton with acetonitrile consisted of all products of four Hermite functions of which the sum of the orders did not exceed 12, yielding a total number of 1820 basis functions. We tested several basis set sizes and concluded that there is very little difference between a spectrum computed with a $10 \times 10 \times 10 \times 10$ basis and one computed with a $12 \times 12 \times 12 \times 12$ basis, indicating that the basis set is almost converged. However, there will be no convergence of the computed spectra for much larger basis sets because the potential has no absolute minimum: it has a negative fourth-order coefficient in the OH stretch coordinate.

The 12 × 12 × 12 × 12 basis set therefore seems best to describe the wave functions in the local minimum of our potential, which corresponds to the minimum in the *real* potential. For consistency we also applied a 12 × 12 × 12 basis in the three-dimensional calculations, with a total of 455 basis functions.

We computed the integrated infrared absorption intensities applying Fermi's golden rule[26] and fractional Boltzmann occupation numbers at a given temperature. The integrated absorption intensities then are given by

$$A_{i\rightarrow f} = \frac{2\pi^2 \Delta E}{3\epsilon_0 h^2 c^2} [|\langle i|\mu_x|f\rangle|^2 + |\langle i|\mu_y|f\rangle|^2 + |\langle i|\mu_z|f\rangle|^2] \frac{e^{-E_i/kT}}{\sum_j^N e^{-E_j/kT}} \quad (4)$$

In this expression the $A_{i\rightarrow f}$ is the absorption intensity for one particle per unit surface, integrated over wave numbers and averaged over different molecular orientations, of the transition between initial level i and final level f, ϵ_0 is the electrical permittivity of vacuum, c is the speed of light, ΔE is the difference in energy between the normalized vibrational states $|i\rangle$ and $|f\rangle$, μ_x, μ_y, and μ_z are the components of the dipole operator, E_j is the energy of vibrational level j, k is the Boltzmann constant, h is the Planck's constant, T is the absolute temperature, and N is the number of levels considered. In the computation of the transition dipoles $\langle i|\mu|f\rangle$ we have taken both *mechanical anharmonicities* (i.e., third order and higher terms in the potential energy) and *electric anharmonicities* (i.e., second order and higher in the dipole) into account. Of these, the mechanical anharmonicities are of far greater influence.

The energy and dipole operators were converted into a representation of annihilation and creation operators,[24] to facilitate analytical computation of matrix elements. The vibrational Hamiltonian eigenvalues and eigenvectors were computed using a Lanczos algorithm,[27,28] with typically 400 iterations for the three-dimensional computations and 2400 for the four-dimensional computations. The described method was implemented in the AnharmNd program, consisting of ±6000 lines of C++ code. SVD and Lanczos routines from the Meschach numerical linear algebra library in C were used.[29]

Results and Discussion

Acidic Proton without Acetonitrile. In the geometry optimizations of the zeolite cluster, we have imposed through symmetry restrictions that the acidic proton should stay in the mirror plane of the cluster. We have computed analytical force constants of the optimized structure and found that the force constant of the out-of-plane bending coordinate corresponded to a very low harmonic frequency of 251 cm^{-1}. The fourth-order polynomial *fit* of the potential energy showed a *maximum* in the energy for our optimized structure and a minimum for a proton position at a distance of 0.254 Å (using DFT) from the mirror plane. The low value of the out-of-plane bending force constant and the fact that our fit yields a negative second derivative in this direction show that the potential energy surface is very shallow around the minimum and is poorly described by a harmonic potential. In solving the Schrödinger equation, one has to integrate the potential energy over the spatial coordinates. Since the fit describes a extended area of the potential energy, it is better suited for the calculation of spectra than the analytical force constant in the minimum of the potential, which only describes the energy in a very small area. Since the Hamiltonian we employed is symmetrical with respect to the mirror plane of the cluster, the vibrational states are symmetric or antisymmetric with respect to the mirror plane. To interpret the calculated states meaningfully in terms of stretch and bending modes, we have performed the calculations with a set of basis functions centered around the proton position of minimum energy in the mirror plane of the zeolite cluster. Because the fit of the energy had a maximum in the point with respect to the out-of-plane bending coordinate, we could not use its curvature in that direction to determine the force constant associated with the Hermite functions. To find a good value for this force constant we have done a calculation in which the Hermite functions have been centered around one of the two proton positions for which the energy polynomial had a minimum. From this calculation we have taken the root mean square displacement of the ground state in the out-of-plane bending coordinate and computed the force constant that a Hermite function with the same width would have. The numerical results of the calculations with the two differently centered basis sets were not noticeably different. In general, it is found that the value of the force constant associated with a basis function can be varied considerably without seriously affecting the results of the lower levels, provided that the basis set used is not very small.

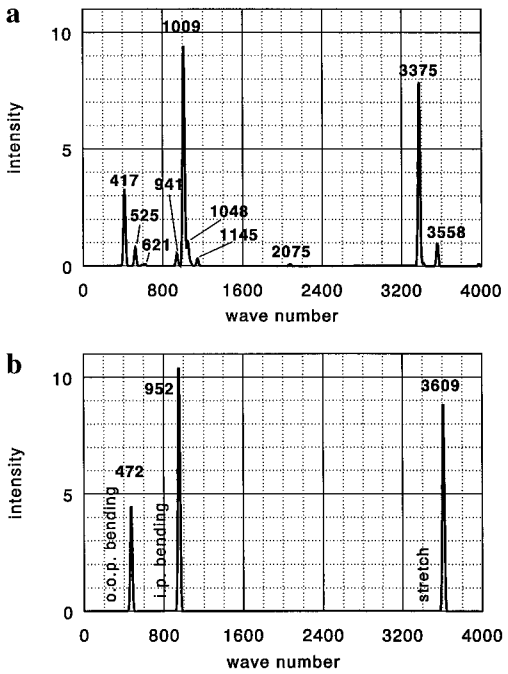

Figure 2. Computed spectra of zeolite acidic proton, at $T = 298.15$ K. Wavenumbers are in cm^{-1}; intensity is in 10^5 m^2/mol. Potential energy and dipole surfaces were computed using DFT. (a) is the computed spectrum including anharmonicities; (b) is computed in the double-harmonic approach.

For the acidic proton we have calculated the 20 vibrational states with lowest energy and the absorption spectrum at a temperature of 298.15 K. We have computed integrated absorption intensities, but no peak widths; the spectra shown in Figures 2 and 3 have been obtained by convolution of Dirac delta functions with normalized Gaussian curves of width 10 cm^{-1}. This means that peak positions and peak surfaces are numerically correct, but peak widths are arbitrary. Table 3 shows the frequencies, integrated absorption intensities, and assignments of the most important transitions in the spectrum. For the DFT potential energy a comparison is given with values obtained by the double-harmonic approach, in which a harmonic potential energy surface and a linear dipole surface are employed. For the double-harmonic calculation we have placed the coordinate origin on one of the proton positions that

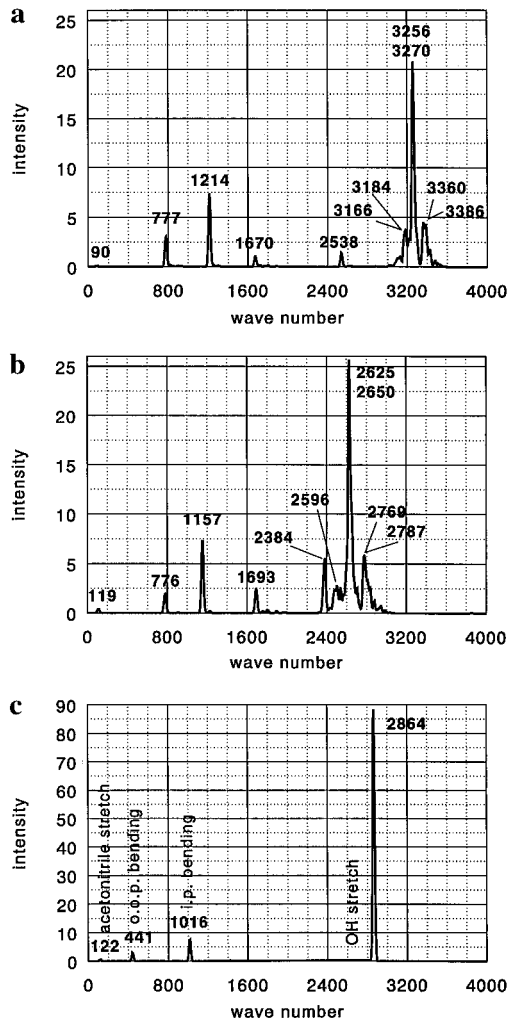

Figure 3. Computed spectra of a zeolite acidic proton interacting with a molecule of acetonitrile, at $T = 298.15$ K. Wavenumbers are in cm^{-1}; intensity is in 10^5 m^2/mol. Spectrum (a) is computed using an SCF potential energy and dipole surface; spectra (b) and (c) are based on DFT data. The spectra (a) and (b) are computed including anharmonicities; spectrum (c) is computed in the double-harmonic approach.

represent a minimum in the potential energy, to avoid computing an imaginary out-of-plane bending frequency.

In the following discussion we will denote vibrational transitions by two sets of quantum numbers separated by an arrow: 123 → 234 denotes a transition from a vibrational state that is once excited in the OH stretch mode, twice in the in-plane bending mode, and three times in the out-of-plane bending mode, to a vibrational state that is one level higher excited in each mode.

In Figure 2 the computed spectra derived from the DFT surfaces are shown. The SCF spectra contain the same transitions, but with higher frequencies, which is due to the fact that SCF overestimates force constants. Comparing the anharmonic calculation with the harmonic result, the OH stretch frequencies are lower, the in-plane bending frequencies are higher, and the out-of-plane bending frequency is higher for the SCF calculation and lower for the DFT calculation. Due to anharmonicity of the out-of-plane bending, the difference in energy between the subsequent excited levels increases, as shown by the transitions at 417 cm^{-1} (000 → 001), 525 cm^{-1} (001 → 002), and 621 cm^{-1} (002 → 003). This is caused by positive quartic terms in the potential energy that render the walls of the potential steeper. Transitions like 001 → 002 and 002 → 003 are, of course, only visible because of thermal population of the excited levels.

TABLE 3: Computed IR Spectrum of the Acidic Proton without Acetonitrile, at $T = 298.15$ K[a]

SCF anharmonic		DFT anharmonic			DFT double harmonic	
ν (cm^{-1})	A (km/mol)	ν (cm^{-1})	A (km/mol)	assignment	ν (cm^{-1})	A (km/mol)
478	110.6	417	81.7	000 → 001	472	89.2
571	20.8	525	20.0	001 → 002	472	18.3
667	1.5	621	1.8	002 → 003	472	2.8
1049	9.9	941	13.0	000 → 002	945	0.0
1126	208.2	1009	236.4	000 → 010	952	229.8
1172	17.1	1048	25.9	001 → 011	952	23.5
1239	5.4	1145	8.0	001 → 003	945	0.0
2308	3.0	2075	2.0	000 → 020	1904	0.0
3779	222.6	3375	197.5	000 → 100	3609	197.4
3975	20.6	3558	25.2	001 → 101	3609	20.2

[a] The assignment column shows the quantum numbers of the basis function with the largest coefficient for the involved states; the first quantum number refers to the OH stretch, the second to the in-plane bending, and the third to the out-of-plane bending. ν is the absorption frequency, A the infrared integrated absorption intensity. For the DFT potential energy surface the transitions in this table with nonzero intensity are indicated in Figure 2.

Also visible due to thermal population, is the 001 → 101 transition at 3558 cm^{-1}. It is higher in frequency than the 000 → 100 transition at 3375 cm^{-1}, because if the out-of-plane bending mode is excited once, the effective Hamiltonian for the OH stretch mode gets a larger second derivative, compared to the ground state.

In the anharmonic spectrum overtones of the out-of-plane bending at 941 cm^{-1} and of the in-plane bending at 2075 cm^{-1} are visible, but clearly much weaker than the fundamentals.

Comparing the results with experimental values for zeolite acidic sites, the DFT OH stretch frequency is low: 3375 cm^{-1} compared to ca. 3600 cm^{-1} found in experiments. There may be various reasons for this. Most important is the fact that we did not allow the oxygen atom to which the acidic proton is attached to move. If this oxygen were not fixed, the resulting reduced mass for the OH stretch mode would be lower, and its absorption frequency would be higher. Also coupling of lower frequency SiO and AlO stretch modes with the OH stretch mode can cause an increase in the OH stretch frequency. Furthermore, the chosen cluster model and the used DFT method may influence the frequencies computed. It was shown earlier that the proton abstraction energy of zeolite clusters similar to the one we used only becomes cluster independent if the cluster represents a substantially larger part of the zeolite.[30] It is not the aim of the present article to resolve this problem. Since further investigation of the effect of the used basis set, and of full geometry optimization, would give more information only about the zeolite cluster we used, we did not pursue this in greater detail. To check whether the DFT method applied could be the cause of the low stretch frequency, we have done a test calculation computing the OH stretch frequency of a silanol group, in a simple one-dimensional approach. We performed a geometry optimization of a $Si(OH)_4$ molecule, employing a 6-31G** basis set, and the same DFT method as in our previous calculations. Five points of the potential energy surface have been computed, expanding one of the (equivalent) OH bonds around the center of mass of the OH group, by factors of 0.8, 0.9, 1.0, 1.1, and 1.4. This is the same as the grid used for the OH stretch mode, the difference being that the oxygen position was not kept fixed this time. Fitting the potential energy with a fourth-order polynomial, we have found a stretch frequency of 3641 cm^{-1}. Adding one point of the potential energy where the OH bond was stretched by a factor of 1.25 yielded a frequency of 3709 cm^{-1}. This is in good agreement with the

TABLE 4: Computed IR Spectrum of the Acidic Proton with Acetonitrile, at $T = 298.15$ K[a]

SCF anharmonic ν (cm^{-1})	DFT anharmonic ν (cm^{-1})	assignment	DFT double harmonic ν(cm^{-1})
90	119	0000 → 0001	122
(774)	776	0001 → 0011	441
777	(783)	0000 → 0010	441
1214	1157	0000 → 0100	1016
1670	1693	0000 → 0020	(883)
2538	2384	0000 → 0200	(2031)
(2708)	2596	0000 → 0202	(2275)
3166	(2507)	0001 → 1000	(2742)
3184	(2395)	0002 → 1001	(2742)
3256	2625	0000 → 1000	2864
3270	2650	0001 → 1001	2864
3360	2769	0000 → 1001	(2986)
(3362)	2787	0001 → 1002	(2986)
3386	(2811)	0002 → 1003	(2986)

[a] The assignment column shows the quantum numbers of the basis function with the largest coefficient for the involved states; the first quantum number refers to the OH stretch, the second to the in-plane bending, the third to the out-of-plane bending, and the fourth to the acetonitrile stretch. ν is the absorption frequency. All wave numbers not in parentheses are printed in Figure 3. The values in parentheses represent transitions of little or no absorption intensity.

experimental value of ca. 3750 cm^{-1} quoted in ref 31 and shows that the density functional method applied is valid for our purposes. Seeing this result, one might think that adding the "1.25 point" may improve our calculations of the acidic site also. This turned out not to be the case. The reason is probably that the potential had already been sampled better, because the bending modes of the proton had been taken into account. Due to interference of lattice modes, OH bending modes in zeolites are experimentally not directly discernible. In the present paper, however, we have tried to describe the dynamics of a hydrogen bond to gain some physical understanding of the involved phenomena, and we have not tried to get quantitative agreement with experiment.

Acidic Proton with Acetonitrile. In the vibrational calculations of the acidic proton with acetonitrile we have computed 120 levels. It has been necessary to compute many more levels than in the three-dimensional case, because the added acetonitrile stretch mode is much lower in frequency than the proton modes, resulting in a large number of levels lower in energy than the first excited OH stretch level. For these calculations the proton position in the mirror plane of the cluster does represent a minimum in the potential energy.

The spectra computed for the acidic proton with acetonitrile adsorbed are shown in Figure 3. In this figure also the SCF spectrum is shown, because it differs in a qualitative way from the DFT spectrum. The differences between the anharmonic and the double-harmonic spectra are much larger than in the spectra of the proton alone. An important contribution to this difference stems from the strong anharmonic coupling between the OH stretch and the acetonitrile stretch, through which many combination bands become visible in the infrared spectrum and give the impression of a broadened OH stretch band. In Table 4 the assignments are given for the most important peaks in the spectra. We did not list integrated absorption intensities, because most of the visual peaks are a superposition of transitions of which the low and high level differ the same number in the excitation level of the acetonitrile stretch; there are more than 100 transitions that give a substantial contribution to the visible bands. Among the transitions that give substantial contributions, i.e., at least 1−10 km/mol, the acetonitrile stretch may be excited as high as to the seventh level.

TABLE 5: Frequency Shifts upon Acetonitrile Adsorption[a]

	stretch	in-plane bending	out-of-plane bending
SCF anharmonic	−523	+88	+299
SCF harmonic	−527	−36	+24
DFT anharmonic	−760	+148	+359
DFT harmonic	−745	+64	−31

[a] Frequency differences in cm^{-1}.

Again it is seen that the anharmonic calculations generate a lower OH stretch frequency compared to the harmonic calculations. All bending frequencies are higher in the anharmonic calculations, and this effect is particularly strong for the out-of-plane bending, which almost doubles in frequency compared to the harmonic calculations.

A very marked change occurring upon acetonitrile adsorption is the increase in infrared absorption intensity. Note the different scales used on the intensity axes comparing Figures 2 and 3. This is caused by enhanced polarization of the OH bond. For the DFT dipole surface, the component of the dipole in the direction of the OH bond is −0.48 ea_0 for the zeolite cluster without acetonitrile and 2.15 ea_0 for the zeolite cluster with acetonitrile. The gradient of the dipole in the OH bond direction increases from 0.46*e* to 1.52*e* upon acetonitrile adsorption. Because the dominant term in the infrared absorption intensity of a transition between two adjacent OH stretch levels contains the square of this gradient, an increase of the intensity by roughly a factor of 10 is to be expected. This is seen most clearly comparing the harmonic spectra in Figures 2 and 3, because they have all intensity due to the OH stretch concentrated at a single wavenumber, whereas in the anharmonic spectra it is spread over a greater number of peaks.

The changes in the infrared spectrum brought about by acetonitrile adsorption are considerably larger for the DFT calculation than for the SCF calculation. This confirms our expectation that the DFT potential energy surface should yield a spectrum that is closer to experiment. In Table 5 the frequency shifts of the OH stretch and bendings are given. The shift of the OH stretch appears to be not very sensitive to anharmonicities. The upward shifts of the bendings are much larger in the anharmonic calculations.

In the following discussion transitions between vibrational states are denoted in the same way as in the previous section, with a fourth quantum number added to describe excitations in the acetonitrile stretch mode. In the four-dimensional calculations the overtones of the out-of-plane bending are visible with enhanced intensity at 1670 cm^{-1} (SCF) and 1693 cm^{-1} (DFT). In the calculation with the SCF potential, the main OH stretch (0000 → 1000) peak at 3256 cm^{-1} is flanked by difference (0001 → 1001) and combination (0000 → 1001) bands with the acetonitrile stretch mode and separate from the overtone of the in-plane bending at 2538 cm^{-1}. In the four-dimensional DFT calculation the main OH stretch peak at 2625 cm^{-1} is flanked on the high-frequency side by combination bands with the acetonitrile stretch, whereas on the low-frequency side the overtone of the in-plane bending and this overtone combined with a doubly excited acetonitrile stretch yield the most important peaks (0000 → 0200 and 0000 → 0202). The latter peaks have a relatively large intensity due to the fact that the strongly absorbing OH stretch mode mixes with the in-plane bending overtone vibrational states. This happens because the frequencies of the OH stretch and the in-plane bending overtone are moving into each other's direction upon acetonitrile adsorption: the in-plane bending mode moves to a higher frequency because acetonitrile pulls the proton in the direction of the mirror plane of the cluster, and the OH stretch frequency decreases

TABLE 6: Largest Coefficients of Basis Functions of Four Vibrational States[a]

2384 cm^{-1}		2586 cm^{-1}		2625 cm^{-1}		2650 cm^{-1}	
function	coefficient	function	coefficient	function	coefficient	function	coefficient
0200	+0.880	0202	+0.637	1000	−0.728	1001	+0.669
1000	−0.285	0203	+0.367	0201	+0.266	1000	+0.344
0220	−0.230	1000	−0.235	0200	−0.242	1002	−0.272
0400	−0.177	1001	+0.234	1001	+0.219	0201	+0.223
0201	+0.091	1002	−0.227	0202	−0.199	0202	−0.222

[a] Of four frequencies in Table 4 the largest coefficients of basis functions of the higher level of the transition are given. The basis functions are labeled by the order of Hermite function of OH stretch, in-plane bending, out-of-plane bending, and acetonitrile stretch coordinate, respectively. The coefficients of the basis functions are normalized, as well as the basis functions themselves.

because the interaction with acetonitrile weakens the OH bond. The SCF potential energy surface reproduces this effect less well, so that there is not much mixing of the OH stretch mode with the in-plane bending overtone, causing the intensity of the 0000 → 0200 transition at 2538 cm^{-1} (Figure 3) to have a much smaller value than the corresponding peak in the DFT spectrum. The interaction of the OH stretch and the overtone of the in-plane bending in the DFT calculation can also be seen from the coefficients of the basis functions in the vibrational wave functions that represent the excited states of the peaks at 2384, 2596, 2625, and 2650 cm^{-1}. These coefficients are listed in Table 6. All the states listed appear to be mixtures of OH stretch and in-plane bending overtone modes.

Pelmenschikov *et al.*[6] suggested that the bands observed at ca. 2800 and 2400 cm^{-1} in the experiment were due to a Fermi resonance between a very strongly broadened OH stretch band ($\nu_{1/2} \approx 800$ cm^{-1}) and a rather sharper in-plane OH bending overtone. That would imply that the maxima correspond to combinations of these modes. In our present results we do find peaks at 2625 and 2384 cm^{-1} that are combinations of OH stretch and in-plane bending overtone. However, the difference in frequency is smaller than in the experiment, and the difference in intensity is much larger than in the experiment; the experimental bands are approximately equally intense. Apparently, the interaction between the OH stretch and the in-plane bending mode in our model is less strong than experimentally. In our model the OH stretch frequency should still get somewhat lower, or the in-plane bending overtone frequency should get somewhat higher, or both. In other words, the proton in our cluster model calculation does not interact strongly enough with acetonitrile; it is not acidic enough. In the following we will first discuss the effect of the acetonitrile stretch mode and the in-plane bending mode on the spectrum and then try to improve on our model, in order to describe and explain the experimental spectrum.

To check the influence of the acetonitrile stretch and the in-plane bending mode of the acidic H, we did calculations with these modes fixed. The results are shown in Figure 4. If we compare the spectrum computed with the acetonitrile stretch fixed with the spectrum with no modes fixed, we see that coupling of the OH stretch mode with the acetonitrile stretch mode is a good candidate as a cause of the broadening of the band. The intensity of the OH stretch is "smeared" out over a wider frequency range. The spectrum where the in-plane bending is fixed allows for study of the interaction of the acetonitrile stretch only, without interference of the in-plane bending overtone. There we see that the main OH stretch adsorption band is flanked by difference and combination bands of the OH stretch mode with the acetonitrile stretch mode. Only transitions that differ one excitation level in the acetonitrile stretch have a substantial contribution. From the spectrum a guess of the half-width of the broadened OH stretch band could be made of 2754 −2469 cm^{-1} = 285 cm^{-1}. In earlier explanations of the phenomenon,[3,5,6] it was assumed that the

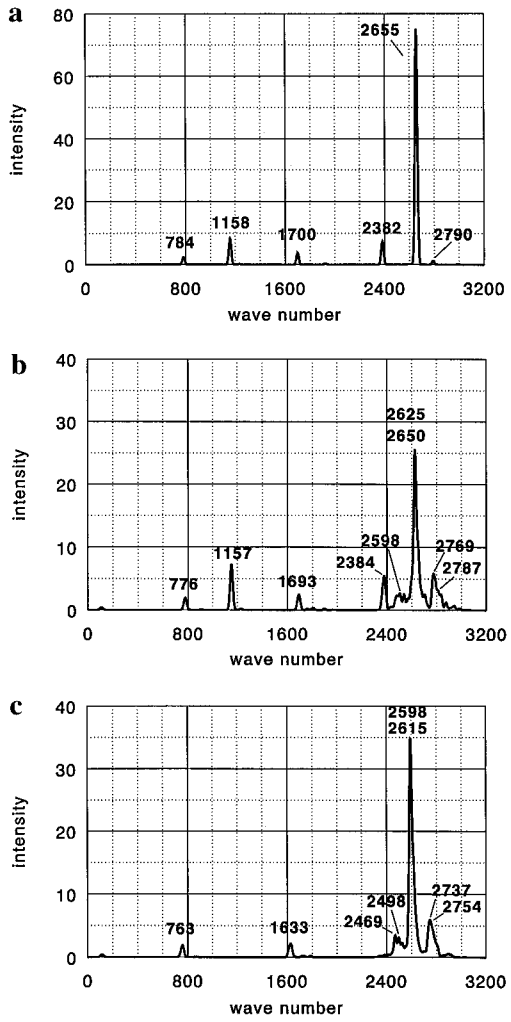

Figure 4. Influence of the OH in-plane bending and the acetonitrile stretch on the spectrum of the acidic proton with acetonitrile. All spectra are computed from DFT potential energy and dipole surfaces, at $T = 298.15$ K, including anharmonicities. Wavenumbers are in cm^{-1}; intensity is in 10^5 m^2/mol. In spectrum (a) the acetonitrile stretch mode is fixed; in spectrum (c) the in-plane bending mode is fixed. For comparison spectrum (b) is plotted, without any modes fixed.

OH stretch band was broadened to a width that comprises both mixed bands, through a coupling of the OH stretch mode with the acetonitrile stretch. This implies for the current system that, in order to reach the width of 800 cm^{-1} suggested in ref 6, the OH stretch mode should yield visible combination bands with the acetonitrile stretch up to the third or fourth excited level: from 0003 → 1000 or 0004 → 1000, to 0000 → 1003 or 0000 → 1004. As an alternative explanation for the experimental spectrum we suggest that there is a resonance of the in-plane bending overtone with an OH stretch band, resulting in two vibrational states that both are mixtures of the two modes. A

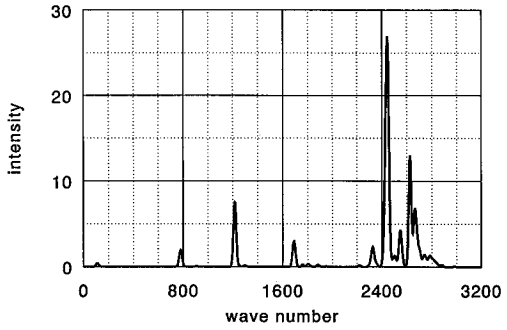

Figure 5. Computed spectrum of a zeolite acidic proton interacting with a molecule of acetonitrile, at $T = 298.15$ K, including anharmonicities. Wavenumbers are in cm^{-1}; intensity is in 10^5 m^2/mol. The DFT potential energy surface was stretched in the OH stretch coordinate and compressed in the in-plane bending coordinate, by a factor of 1.05. The unscaled DFT dipole surface was used.

broadening on the order of 300 cm^{-1} is seen in both mixed mode bands, at 2400 and 2800 cm^{-1}.

In an attempt to render our model somewhat more "acidic", we have modified the DFT potential. We have stretched it in the OH stretch coordinate, making the potential flatter to lower the OH stretch frequency, and at the same time compressed it by the same scale factor in the in-plane bending coordinate, making it steeper to increase in the in-plane bending frequency. In Figure 5 the spectrum that is obtained by application of a scale factor of 1.05 is shown. This spectrum very much resembles the experimental spectra, showing two main broadened bands that are due to combinations of the in-plane bending overtone and the OH stretch mode. The most significant difference with the experimental spectra is the distance between the two peaks, which is smaller in the computation.

A deeper insight in the nature of the resonance can be gained by looking at the frequencies and intensities of the two peaks as a function of the acidity, modeled by the aforementioned scale factor. In Figure 6 we have plotted this for our model of the acidic OH, where the acetonitrile was kept at a fixed position, so that absorption intensity could be unambiguously attributed to one of the two main peaks. Going from the left to the right in Figure 6 the potential becomes flatter in the OH stretch direction and steeper in the in-plane bending direction. In the upper part of the graph the frequencies of the high- and the low-frequency band are plotted. In the lower part the corresponding relative intensities are shown. At low acidity (scale factor 1) the high-frequency band, which has more OH stretch character, has the largest intensity, and the low-frequency band, which has more in-plane bending overtone character, has relatively small intensity. At the strongly acidic side of the graph (scale factor 1.1) the situation is reversed: the low-frequency band has more OH stretch character and also the largest absorption intensity. The complete graph can be viewed as a forbidden crossing: with increasing acidity the OH stretch frequency is lowered, and the in-plane bending overtone frequency increases. Somewhere halfway the graph of the two modes would have the same frequency, if they did not couple. Since they do couple, the levels are split. The frequency of decoupled OH stretch and in-plane bending overtone modes can be computed assuming that all of the infrared absorption intensity is due to the OH stretch mode. This is a fairly accurate assumption for the given system. The derivation of the formulas used to compute the decoupled frequencies plotted in Figure 6 is given in the Appendix.

Figure 6 shows that in a certain range of different scale factors the frequencies of the two main peaks due to hydrogen bonding do not vary strongly, whereas the intensity is transferred from

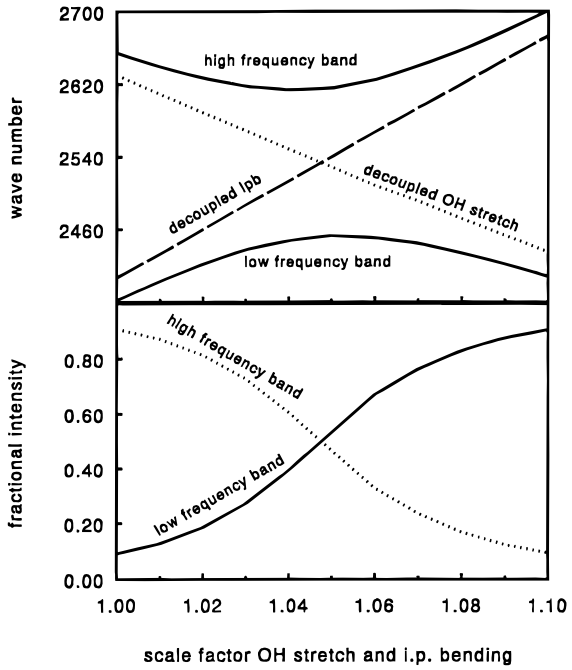

Figure 6. Frequency and intensity of the two main adsorption bands in the spectrum of the zeolite acidic proton interacting with a molecule of acetonitrile as a function of a scale factor, at $T = 298.15$ K. Wavenumbers are in cm^{-1}; intensity is in 10^5 m^2/mol. The scale factor is the factor by which the DFT potential energy was stretched in the OH stretch coordinate and compressed in the in-plane bending coordinate. This simulates a more acidic OH group for larger scale factors. The frequencies and intensities were computed keeping the acetonitrile stretch mode fixed. The upper part of the graph shows the wavenumbers of the two bands; the lower part shows their intensities, relative to the total intensity of both bands. Further explanation is given in the text.

the high-frequency band to the low-frequency band. This transfer of intensity is illustrated by Figure 7, which shows the spectra corresponding to the left, middle, and right of Figure 6. The position of the dip between the two bands, defined as the average of the frequencies of the two bands, stays approximately the same in the whole range of scale factors tested and corresponds to the place where the decoupled OH stretch and in-plane bending overtone cross each other.

In Figure 8 the computed spectrum (scale factor 1.05) of the acidic proton with acetonitrile is shown both at room temperature (298.15 K) and liquid nitrogen temperature (77 K). The most marked difference is the fact that at low temperature the absorption intensity is concentrated in fewer peaks. Cooling down to even lower temperatures (liquid helium, 4.2 K) doesn't make much further difference. For the modes we studied it appears as though measurements at low temperature might give a better resolution, but the experimental spectrum could still be blurred by coupling of lattice modes and inhomogeneous line broadening. In the computed spectra also some broadening of the two-band system is observed when going to a higher temperature.

An interesting, though small, temperature effect is that the overall intensity of the spectrum decreases by 3.43% going from 77 to 298.15 K (computed with the unscaled potential energy). This is probably due to the larger distance between the OH group and the acetonitrile molecule at higher temperatures, which results in a smaller interaction. Taking into account the Boltzmann distributions over the different vibrational levels, we have computed the average distance between acetonitrile and the O atom of the OH group to grow by 0.027 Å going from 77 to 289.15 K (again for the unscaled potential).

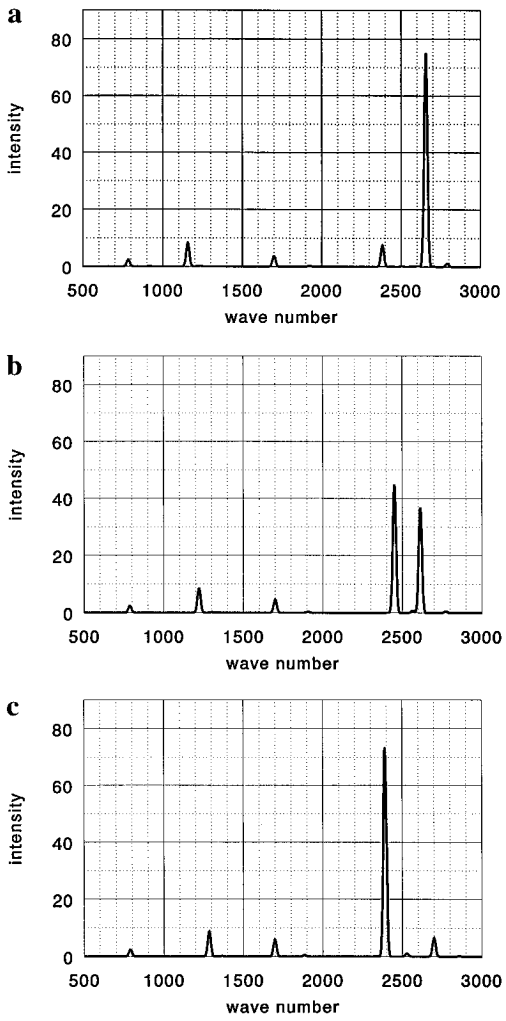

Figure 7. Computed spectra of a zeolite acidic proton with acetonitrile, with acetonitrile fixed at the equilibrium position, at $T = 298.15$ K. Wavenumbers are in cm^{-1}; intensity is in 10^5 m^2/mol. The spectra are based on the DFT potential energy and dipole surface; they differ in scale factor for the OH stretch and in-plane bending modes. Spectrum (a) has a scale factor of 1.00, spectrum (b) has a scale factor of 1.05, and spectrum (c) has a scale factor of 1.10. The scaled potential energy surfaces model zeolite OH groups that are more acidic going from (a) to (c). The spectra correspond to the left, middle, and right of Figure 6.

Conclusions

The experimentally observed splitting of OH stretch infrared absorption bands upon adsorption of a basic molecule can be explained by the interaction of the OH in-plane bending overtone with the OH stretch mode. The two main absorption bands seen in experiment are both due to differently mixed in-plane bending and OH stretch modes.

More acidic OH groups have a relatively more intense low-frequency OH stretch absorption band, compared to the high-frequency band, if a basic molecule is absorbed. The dip between the two main absorption bands is approximately at the position where the decoupled OH stretch and in-plane bending mode would cross each other with increasing acidity.

The used $(HO)_3Al(OH)Si(OH)_3$ zeolite cluster seems to be not "acidic" enough if, at DFT level, only the H atom is allowed to move. This may be due to the limited number of degrees of freedom considered and to shortcomings of the cluster molecule as a model of the zeolite. From a test calculation of the silanol OH stretch frequency it appears that the applied DFT method is valid for the computation of infrared spectra.

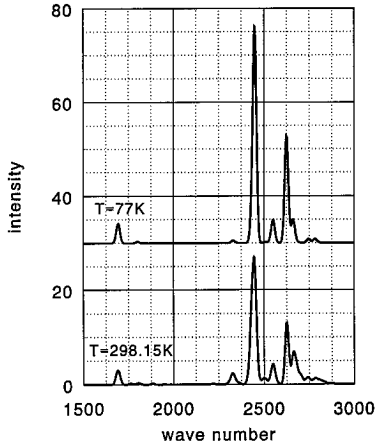

Figure 8. Computed spectra of a zeolite acidic proton interacting with a molecule of acetonitrile, at $T = 77$ K and at $T = 298.15$ K. Wavenumbers are in cm^{-1}; intensity is in 10^5 m^2/mol. The spectra are computed using DFT (scale factor 1.05) potential energy and dipole surfaces.

Acknowledgment. E.L.M. gratefully acknowledges financial support by Shell laboratories in Amsterdam (KSLA) for the beginning of his graduate research.

Appendix: Derivation of Decoupled Mode Frequencies

The OH stretch and overtone in-plane bending modes are strongly coupled if there is hydrogen bonding to a molecule of acetonitrile. In this paper we estimated the frequencies of the decoupled modes in a way that can be applied to experimental data as well. The formulas used to compute the frequencies are deduced as follows.

Let $|\phi_0\rangle$ be the vibrational ground state and $|\phi_1\rangle$ and $|\phi_2\rangle$ the mixed states of OH stretch and the overtone of the in-plane bending that occur as eigenstates of the Hamiltonian. Let $|\psi_1\rangle$ be the decoupled excited OH stretch state and $|\psi_2\rangle$ the decoupled doubly excited in-plane bending state. The coupled states can be written as linear combinations of the decoupled states:

$$|\phi_i\rangle = \sum_j c_{ij}|\psi_j\rangle \tag{5}$$

where $\{c_{ij}\}$ are the coefficients of an orthogonal 2×2 matrix. In good approximation it can be assumed that the absorption intensity of the transitions between the ground state and $|\phi_1\rangle$ and $|\phi_2\rangle$ is entirely due to the OH stretch mode. Therefore, we can write for the transition dipole moments:

$$\langle\phi_0|\mu_\alpha|\phi_i\rangle = \sum_j c_{ij}\langle\phi_0|\mu_\alpha|\psi_j\rangle = c_{i1}\langle\phi_0|\mu_\alpha|\psi_1\rangle \equiv c_{i1}p_\alpha, \quad \alpha = x, y, z \tag{6}$$

where μ_α are the dipole operator components. The absorption intensity A_i of the transition from $|\phi_0\rangle$ to $|\phi_i\rangle$ is proportional to the square of the transition dipole moment and the energy difference between the involved states, so that

$$A_i \propto (\epsilon_i - \epsilon_0)\sum_\alpha |\langle\phi_i|\mu_\alpha|\phi_0\rangle|^2 = (\epsilon_i - \epsilon_0)c_{i1}{}^2\sum_\alpha p_\alpha{}^2 \tag{7}$$

where ϵ_i denotes the eigenvalue of $|\phi_i\rangle$. For the relative intensities we can write, using $c_{21}{}^2 = 1 - c_{11}{}^2$ (from the orthogonality of the transformation matrix):

$$\frac{A_1}{\sum_i A_i} = \frac{(\epsilon_1 - \epsilon_0)c_{11}^2\sum_\alpha p_\alpha^2}{(\epsilon_1 - \epsilon_2)c_{11}^2\sum_\alpha p_\alpha^2 + (\epsilon_2 - \epsilon_0)\sum_\alpha p_\alpha^2} = \frac{\nu_1}{(\nu_1 - \nu_2) + \nu_2/c_{11}^2} \equiv f_1 \quad (8)$$

where ν_i ($\propto \epsilon_i - \epsilon_0$) is the frequency of the transition $|\phi_0\rangle \rightarrow |\phi_i\rangle$. This enables us to compute c_{11}^2 from information that can be obtained from either an experimental or a computed spectrum:

$$c_{11}^2 = f_1 \frac{\nu_2}{\nu_1 + (\nu_2 - \nu_1)/f_1} \quad (9)$$

Using

$$H|\phi_i\rangle = \epsilon_i|\phi_i\rangle \quad \text{and} \quad |\psi_j\rangle = \sum_k c_{kj}|\phi_k\rangle \quad (10)$$

and the orthogonality of the transformation matrix between the coupled and the decoupled states, we can compute

$$\langle\psi_1|H|\psi_1\rangle = c_{11}^2(\epsilon_1 - \epsilon_2) + \epsilon_2 \quad (11)$$

$$\langle\psi_2|H|\psi_2\rangle = c_{11}^2(\epsilon_2 - \epsilon_1) + \epsilon_1$$

and finally for the frequencies

$$\nu_{|\phi_0\rangle\rightarrow|\psi_1\rangle} = \frac{\nu_2(\nu_1 - \nu_2)f_1}{\nu_1 + (\nu_2 - \nu_1)/f_1} + \nu_2 \quad (12)$$

$$\nu_{|\phi_0\rangle\rightarrow|\psi_2\rangle} = \frac{\nu_2(\nu_2 - \nu_1)f_1}{\nu_1 + (\nu_2 - \nu_1)/f_1} + \nu_1$$

References and Notes

(1) Kubelková, L.; Nováková, J.; Nedomová, K. *J. Catal*. **1990**, *124*, 441.

(2) Mirth, G.; Lercher, J. A.; Anderson, M. W.; Klinowski, J. *J. Chem. Soc., Faraday Trans*. **1990**, *86*, 3039.

(3) Claydon, M. F.; Sheppard, N. *Chem. Commun*. **1969**, 1431.

(4) Odinokov, S. E.; Iogansen, A. V. *Spectrochim. Acta* **1972**, *28A*, 2343.

(5) Sheppard, N. *Hydrogen Bonding*; Hadži, D., Ed.; Pergamon: San Francisco, London, 1960.

(6) Pelmenschikov, A. G.; van Santen, R. A.; Jänchen, J.; Meijer, E. L. *J. Phys. Chem*. **1993**, *97*, 11071.

(7) Becke, A. D. *J. Chem. Phys*. **1993**, *98*, 5648.

(8) Becke, A. D. *Phys. Rev. A* **1988**, *38*, 3098.

(9) Lee, C.; Wang, W.; Parr, R. G. *Phys. Rev. B* **1988**, *37*, 785.

(10) Vosko, S. H.; Wilk, L.; Nusair, M. *Can. J. Phys*. **1980**, *58*, 1200.

(11) Rashin, A. A.; Young, L.; Topol, I. A.; Burt, S. K. *Chem. Phys. Lett*. **1994**, *230*, 182.

(12) Hehre, W. J.; Stewart, R. F.; Pople, J. A. *J. Chem. Phys*. **1969**, *51*, 2657.

(13) Gordon, M. S.; Binkley, J. S.; Pople, J. A.; Pietro, W. J.; Hehre, W. J. *J. Am. Chem. Soc*. **1982**, *104*, 2797.

(14) Hehre, W. J.; Ditchfield, R.; Pople, J. A. *J. Chem. Phys*. **1971**, *56*, 2257.

(15) Francl, M. M.; Pietro, W. J.; Hehre, W. J.; Binkley, J. S.; Gordon, M. S.; Defrees, D. J.; Pople, J. A. *J. Chem. Phys*. **1986**, *77*, 3654.

(16) Hariharan, P. C.; Pople, J. A. *Theor. Chim. Acta* **1973**, *28*, 213.

(17) Kirshnan, R.; Binkley, J. S.; Seeger, R.; Pople, J. A. *J. Chem. Phys*. **1973**, *72*, 650.

(18) Clark, T.; Chandrasekhar, J.; Spitznagel, G. W.; Schleyer, P. v. R. *J. Comput. Chem*. **1982**, *4*, 294.

(19) Defrees, D. J.; McLean, A. D. *J. Comput. Chem*. **1986**, *7*, 321.

(20) Haw, J. F.; Haw, M. B.; Alvaro-Swaisgood, A. E.; Munson, E. J.; Lin, Z.; Beck, L. W.; Howard, T. *J. Am. Chem. Soc*. **1994**, *116*, 7308.

(21) Frisch, M. J.; Trucks, G. W.; Schlegel, H. B.; Gill, P. M. W.; Johnson, B. G.; Wong, M. W.; Foresman, J. B.; Robb, M. A.; Head-Gordon, M.; Replogle, E. S.; Gomperts, R.; Andres, J. L.; Raghavachari, K.; Binkley, J. S.; Gonzalez, C.; Martin, R. L.; Fox, D. J.; Defrees, D. J.; Baker, J.; Stewart, J. J. P.; Pople, J. A. *Gaussian 92/DFT*, Revision F.2; Gaussian, Inc.: Pittsburgh, PA, 1993.

(22) Press, W. H.; Flannery, B. P.; Teukolsky, S. A.; Vetterling, W. T. *Numerical Recipies in C, The Art of Scientific Computing*; Cambridge University Press: Cambridge, 1988; Chapter 2.9.

(23) Wilson, E. B., Jr.; Decius, J. C.; Cross, P. C. *Molecular Vibrations*; Mc-Graw-Hill: New York, Toronto, London, 1955.

(24) Messiah, A. *Quantum Mechanics*; John Wiley & Sons: New York, 1974; Chapter XII.

(25) Mijoule, C.; Allavena, M.; Leclerq, J. M.; Bouteiller, Y. *Chem. Phys*. **1986**, *109*, 207.

(26) Pauling, L.; Wilson, E. B. *Introduction to Quantum Mechanics*; McGraw-Hill: New York, 1935; Chapter XI.

(27) Lanczos, C. J. *J. Res. Natl. Bur. Stand*. **1950**, *45*, 255.

(28) Parlett, B. N. *The Symmetric Eigenvalue Problem*; Prentice-Hall: Englewood Cliffs, NJ, 1980.

(29) Stewart, D. E.; Leyk, Z. *Meschach*: *Matrix Computations in C*: Centre for Mathematics and its Applications, Australian National University: Canberra, 1994.

(30) Brand, H. V.; Curtiss, L. A.; Iton, L. E. *J. Phys. Chem*. **1992**, *96*, 7725.

(31) Pelmenschikov, A. G.; Morosi, G.; Gamba, A. *J. Phys. Chem*. **1991**, *95*, 10037.

JP951164I